Journal of Power Sources 210 (2012) 276–285

Contents lists available at SciVerse ScienceDirect

Journal of Power Sources

journal homepage: www.elsevier.com/locate/jpowsour

Influence of electrode preparation on the electrochemical performance of $LiNi_{0.8}Co_{0.15}Al_{0.05}O_2$ composite electrodes for lithium-ion batteries

Hai Yen Tran [a], Giorgia Greco [a], Corina Täubert [a], Margret Wohlfahrt-Mehrens [a,*], Wolfgang Haselrieder [b], Arno Kwade [b]

[a] ZSW – Zentrum für Sonnenenergie- und Wasserstoff-Forschung, Baden-Württemberg, Helmholtzstrasse 8, D-89081 Ulm, Germany
[b] TU Braunschweig, Institute for Particle Technology, Volkmaroderstrasse 5, D-38104 Braunschweig, Germany

ARTICLE INFO

Article history:
Received 6 January 2012
Accepted 7 March 2012
Available online 21 March 2012

Keywords:
Electrode preparation
$LiNi_{0.8}Co_{0.15}Al_{0.05}O_2$
Lithium-ion
Cathode material

ABSTRACT

The electrode manufacturing for lithium-ion batteries is based on a complex process chain with several influencing factors. A proper tailoring of the electrodes can greatly improve both the electrochemical performances and the energy density of the battery. In the present work, some significant parameters during the preparation of $LiNi_{0.8}Co_{0.15}Al_{0.05}O_2$-based cathodes were investigated. The active material was mixed with a PVDF-binder and two conductive additives in different ratios. The electrode thickness, the degree of compacting and the conductive agent type and mixing ratio have proven to have a strong impact on the electrochemical performances of the composite electrodes, especially on their behaviour at high C-rates. Further it has been shown that the compacting has an essential influence on the mechanical properties of NCA coatings, according to their total, ductile and elastic deformation behaviour.

1. Introduction

Layered oxides such as $LiNiO_2$ and $LiCoO_2$ were discovered more than 20 years ago and intensively investigated as possible cathode materials for electrochemical power sources [1]. $LiCoO_2$ exhibits good electrochemical properties and is therefore still used as cathode material in most of the commercial lithium-ion cells. $LiNiO_2$ has the advantages of being less expensive and less toxic than $LiCoO_2$, but it suffers from difficulties in the synthesis, irreversible phase transitions during cycling, and the so-called Jahn–Teller distortion. Another important issue is the relative low thermal stability of $LiNiO_2$ which can cause safety problems in the delithiated state. All these make $LiNiO_2$ as undesirable cathode material for Li-ion cells. To overcome these shortcomings of $LiNiO_2$, partial cobalt-substitution has been identified as a solution [2]. Sanyo published 2002 a report in which the thermal behaviour of a mixed Ni/Co material $LiNi_{0.7}Co_{0.3}O_2$ was successfully simulated for the design of 2 Wh-class cells for load levelling systems [3].

In order to improve several properties of the layered oxide cathode materials (e.g. safety, cycleability, toxicity, cost) many doping metallic ions have been investigated in the last decade. Among these, aluminium was found as a candidate for improving safety characteristics and cycleability compared to the pure $LiNiO_2$ cathode material [4–6].

In comparison to the efforts concentrated in finding new, better-performing cathode materials for Li-ion batteries, the literature on electrode preparation is scarce. Most of the publications focusing on the design and manufacturing of electrodes are patents [7,8]. Typically, a mixture used for electrode preparation contains as ingredients active material, carbon black for ensuring the electrical conductivity, a binder (mostly polyvinylidene fluoride — PVDF) for holding the powder in a mechanically stable layer and a solvent for adjusting the slurry viscosity.

Generally, the electrode manufacturing for high power/high energy Li-ion batteries requires precision and accuracy and bases on a complex process chain with numerous influencing factors. The most important processing steps are: the selection and, if necessary, the pre-treatment (e.g. drying, milling, etc.) of the ingredients, the mixing ratio and sequence (recipe), the dispersion, the coating onto the current collector, the consequent drying, and calandering. In addition to these operating parameters the particle morphology of the raw materials, the slurry homogeneity, the electrode thickness as well as the mechanical stability and porosity of the electrode composite have also proven to exhibit a strong influence on the electrochemical performance of the electrodes. Therefore, a proper design of the electrodes can greatly improve the energy density, or power density, as well as the cycleability, which are important characteristics in Li-ion batteries. Manabu et al. [9] proposed that a positive electrode for Li-ion batteries should have a thickness between 80 and 250 μm in order to achieve high capacity, high energy density and long-term cycleability. Furthermore, the output density can be improved without affecting the energy density by applying two layers of active material having different

* Corresponding author. Tel.: +49 731 9530 612; fax: +49 731 9530 666.
E-mail address: margret.wohlfahrt-mehrens@zsw-bw.de (M. Wohlfahrt-Mehrens).

0378-7753/$ – see front matter © 2012 Elsevier B.V. All rights reserved.
doi:10.1016/j.jpowsour.2012.03.017

porosities onto the current collector according to Yuji et al. [10]. The porosity of the active material layer at the current collector side is proposed to be between 30% and 50%, and at the separator side between 50% and 60%. The effect of mixing sequence of the starting materials on the characteristics of the final product – i.e. the electrode – as well as the dispersion were reported by Kim et al. [11] and Terashita et al. [12]. Kim et al. achieved an excellent cycling stability of the electrodes by pre-mixing the active material powder with the conductive agent before adding the binder solution and solvent, while Terashita et al. reached a higher energy density by adding a thickening agent in the dispersion. Improved electrode characteristics were obtained also by applying high energy mechanical milling as shown in other two studies [13,14]. It has been also reported that the particle size of the conductive agent (e.g. carbon black, graphite) plays an important role in the performance of the Li-ion cells [15].

In the present work, we have systematically examined in laboratory scale some significant parameters during the preparation of $LiNi_{0.8}Co_{0.15}Al_{0.05}O_2$-based cathodes. Electrode thickness, the degree of compacting and the conductive additive type have proven to have a strong impact on the electrochemical performances of the composite electrodes, especially on their rate capability.

2. Experimental

2.1. Electrode preparation

The composite positive electrodes consisted of $LiNi_{0.8}Co_{0.15}Al_{0.05}O_2$ (NCA from Toda; $D_{50} = 9.7\,\mu m$) as active material, conductive additives and polyvinylidene fluoride binder (PVDF from Solvay Solexis) in the weight ratio 84:8:8. Carbon black (Super P, Timcal) and graphite (SFG6, Timcal) mixed in different ratios were used as conductive agents. Super P and graphite were chosen as two of the most used conductive agents for Li-ion batteries electrodes. *N*-methylpyrrolidone (NMP, from Sigma–Aldrich) was used for preparing the binder solutions. For the electrode preparation, the conductive agents were first mixed in the binder solution under strong stirring to reduce agglomerations. The active material was added only after the conductive agents were homogeneously dispersed in the binder solution. The slurry was further smoothly stirred, while keeping the viscosity under control. The resulting slurry was coated onto aluminium foil (22 μm thickness) using the doctor-blade technique and then dried at 80 °C to evaporate NMP. The film was after that dried overnight at 120 °C under vacuum to evaporate solvent and water residues in the composite electrode.

The wet thickness of the electrodes was varied between 150 μm and 350 μm in order to explore the effect on the electrochemical performance of the electrode. In addition, the applied pressure on the 12 mm diameter electrode was investigated as well.

2.2. Electrode characterization

The slurry viscosity was controlled by using a digital rheometer (Brookfield, model DV-III). Scanning electron microscopy (SEM) – normal and cross-section – was used as a powerful tool to investigate the morphology of the electrodes. The mechanical properties of the electrodes such as adhesion of the coating to the current collector as well as the deformation energy have been investigated by a tape test and by nano-indentation (Triboindenter, Hysitron), respectively. For nano-indentation measurements a flat-ended tip with a diameter of 50 μm was used for load controlled measurements. The electrochemical characterization was carried out in three-electrodes cells, assembled under inert gas atmosphere in an argon-filled glove box (MBraun). Lithium metal was used as reference and counter electrode. Glass microfiber (Whatmann, GF/A) was used as separator. The electrolyte consisted of 1 M $LiPF_6$ in EC:DMC (1:1 by wt., from UBE, Japan). All measurements were carried out at room temperature using a VMP multi-channel potentiostat/galvanostat (Bio-logic Science Instruments), provided with an EC-Lab® software, and a galvanostatic device (BEATE) using a Basytec-type software. The electrochemical technique used in this work was galvanostatic cycling with potential limitation. The cut-off potentials were set at 4.2 and 3.0 V, respectively. All potentials are quoted here versus Li/Li^+.

3. Results and discussion

The effect of three different factors on the electrochemical performance of the electrodes has been investigated: (i) coating thickness; (ii) degree of compacting and (iii) conductive agent type. These three factors are considered from the authors as some of the most relevant, having a significant influence especially on the rate capability of the electrodes. The observed effects can be interpreted by means of the electronic and ionic conductivity within the whole system. In both cases one has to distinguish between material and composite electrode effects.

For the electronic conductivity one has to take into account three main parameters: the conductivity in the primary crystallites of the active material forming the grains, the electronic contact within the grains (active mass–active mass) and the electronic contact within the electrode composite (active mass–carbon, active mass–aluminium foil, carbon–aluminium foil, etc.). The latter can be controlled by a proper electrode design.

Lithium ion diffusion is influenced by crystallite (diffusion coefficient) and grain parameters (grain porosity) as well. In the electrode composite the ion diffusion is governed mostly by the pore distribution which controls the electrolyte access to the active material.

3.1. Wet coating thickness

Slurries containing 84 wt.% NCA, 4 wt.% Super P, 4 wt.% graphite (SFG6) and 8 wt.% PVDF-binder have been prepared and coated onto aluminium foil using different thicknesses between 150 and 350 μm (the thickness is referred to the wet film). The electrodes were after that dried over night at 80 °C and then compacted by using a controlled pressure of 694 MPa. The cross-section SEM micrographs of the compacted electrodes are shown in Fig. 1. The on-aluminium-coated layers are quite smooth and homogeneous. As expected, the electrode loading density has been improved by increasing the thickness.

The correlation between the thicknesses of the wet and dry layers, respectively and the loading density of the non-compacted electrodes is depicted in Fig. 2. One can observe an almost linear correlation wet layer thickness-loading density which could be very helpful in tailoring electrodes for Li-ion batteries with the appropriate properties for the required applications. In order to obtain a reasonable loading density as well as homogeneity of the electrodes a thickness of 150 μm (wet layer) should be considered as the lowest limit.

Furthermore, the surface porosity of the electrodes at different thicknesses has been investigated by analyzing the SEM images with the ImageJ (National Institutes of Health, United States) software [16]. A commonly used relationship between the surface porosity and the electrode thickness is given by the Athy's equation [17]:

$$\phi(z) = \phi_0 e^{-kz} \quad (1)$$

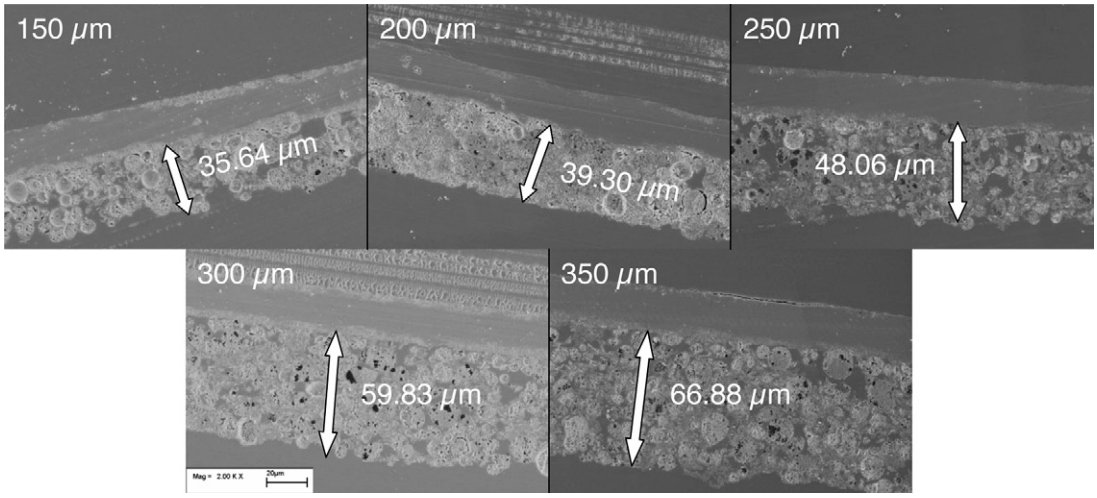

Fig. 1. Cross-section SEM images of compacted NCA-electrodes. The thickness of the wet film has been varied between 150 and 350 μm.

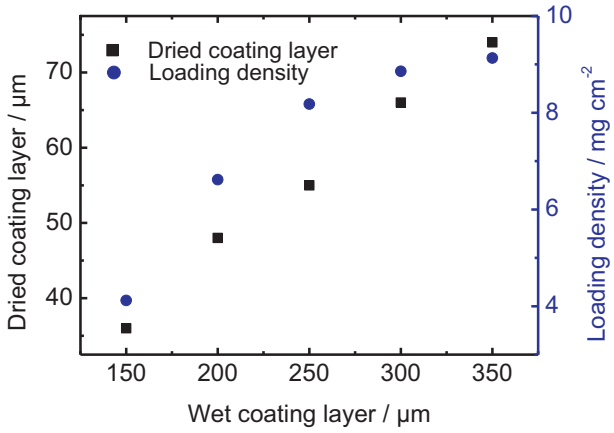

Fig. 2. Correlation wet/dried layer thickness – loading density of the non-compacted electrodes.

with the surface porosity ϕ_0, the electrode thickness z (μm) and the uniaxial compaction coefficient k (μm^{-1}). In the present study k is defined as:

$$k = \frac{ds}{d\varepsilon_z} C_{\text{exp}} \tag{2}$$

where ds is the strain, $d\varepsilon_z$ is the variation caused by stress (see Fig. 3a) and C_{exp} is a correction factor calculated by the experimental evidence ($C_{\text{exp}} = 10^{-15}$).

Fig. 3 shows two SEM images of an electrode (250 μm, wet) at different magnitudes. Differences in pores analysis can be observed. Therefore, the total surface porosity ϕ_0 has been evaluated by the sum of the surface porosity at each magnitude using following formula:

$$\phi_0 = \frac{1}{n}\sum_{n=1}^{N} \phi_{1T}^{(n)} + \frac{1}{m}\sum_{m=1}^{N} \phi_{3T}^{(m)} + \cdots \tag{3}$$

with the image resolution nT ($n = 1, \ldots, N$).

The correlation between the surface porosity of the electrodes and the layer thickness is shown in Fig. 4: the higher the electrode thickness; the lower the surface porosity.

Moreover, the compression coefficient G for different wet electrodes thicknesses has been calculated as well by using following consideration:

$$G = V_0 \frac{\Delta P}{\Delta V} \tag{4}$$

where V_0 is the electrode volume at the beginning, $\Delta V = V_0 - V$ is the electrode volume change after pressing and ΔP is the variation of pressure (694 MPa) (see Table 1). After 250 μm (wet thickness) a constant compression coefficient has been observed. This indicates that the electrodes thicker than 250 μm (wet) will supposably experience similar electrochemical performance at high C-rates.

The influence of the electrode thickness on the rate capability has been studied as well. Fig. 5 shows the discharge capacities of the Li/NCA cells at different C-rates between C/5 and 5C. At relatively

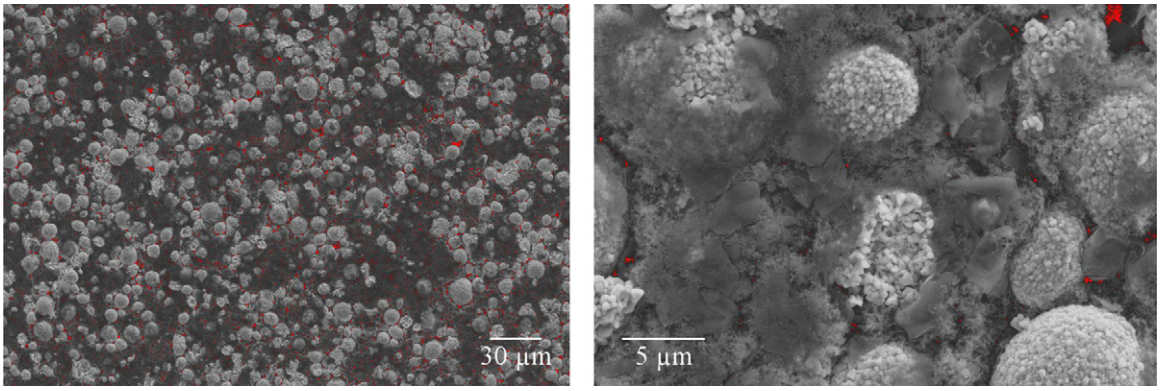

Fig. 3. SEM images of an 250 μm thick electrode with two different magnitudes. The pores are displayed in red. (For interpretation of the references to colour in this figure legend, the reader is referred to the web version of the article.)

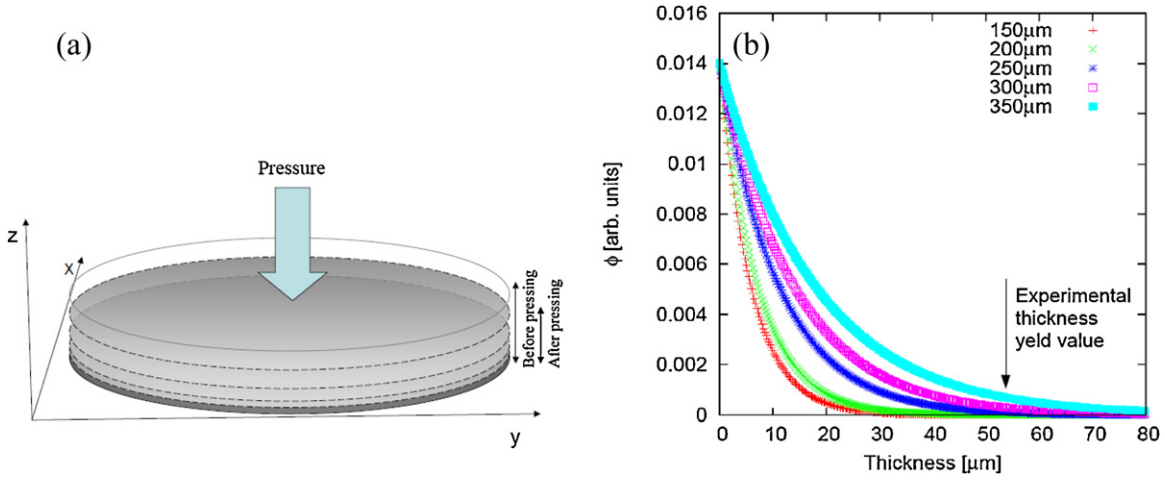

Fig. 4. (a) Schematic view of an electrode and (b) porosity as a function of depth obtained from Athy's equation for different electrodes with a different wet thickness. The pressure exert on the electrode is the same: 694 MPa.

Table 1
Compaction (k) and compression coefficients calculated for the different values of wet electrodes thickness.

Wet thickness [µm]	Dry and pressed thickness [µm]	G [GPa]	k [µm^{-1}]
150	36	2.4(5)	0.175
200	48	3.4(5)	0.142
250	55	3.0(5)	0.090
300	66	3.3(5)	0.072
350	74	3.3(5)	0.056

low current densities no significant differences between the NCA electrodes with different loadings have been observed.

On contrary, at higher C-rates electrodes with lower loading deliver significantly more capacity than those with higher loading. The poor rate capability of the latter can be explained by the longer electron transport paths within the electrode. This results in a higher number of contact resistance points leading to a higher overall electronic resistance. For very high C-rates electrolyte diffusion may become significant and lithium exhaustion can be the rate limiting factor.

An abrupt decrease in the electrochemical performances of the electrodes between 150 and 200 µm can be very well observed. Electrodes with a wet thickness between 250 and 350 µm show similar discharge capacities at C-rates as high as 5C, which is in agreement with the result from the surface porosity analysis.

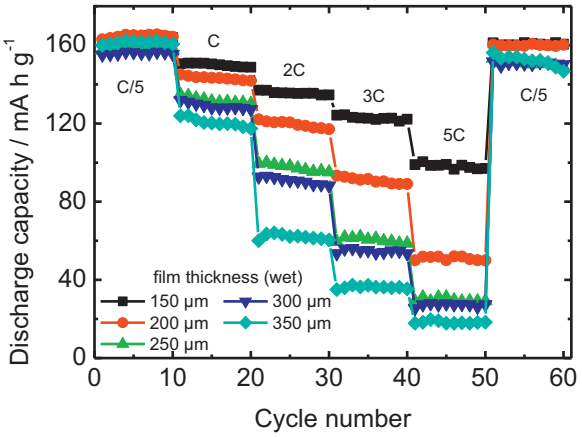

Fig. 5. Electrochemical performance of different thick NCA electrodes. The cut-off potentials were 4.2 and 3.0 V and the charge/discharge rates varied between C/5 and 5C.

Electrodes for Li-ion batteries used for consumer applications should have a thickness of at least 80 µm in the dried state [9]. As Fig. 5b shows, NCA electrodes thicker than 55 µm show a very poor rate capability which makes them not suitable for high power applications. In order to improve their electrochemical behaviour electrode compacting and/or using different conductive agents in different ratios have been investigated.

3.2. Compacting of the electrodes

Electrodes with 250 µm thickness (wet film) were chosen for evaluating the influence of compacting on both thickness and electrochemical performance. At first the impact of compression on the mechanical properties of electrode coatings has been investigated by comparing ductile, elastic and total deformation energies of a non-compacted and a compacted electrode using nano-indentation technique [18]. A compaction degree of 10% (related to the dry electrode composite thickness including current collector) has been analysed in comparison to the non-compacted type of the same batch. Each analysis is based on 25 single indentation measurements applied in a regular pattern on the electrode. Table 2 summarizes the average values and their standard deviation.

The values in Table 2 clearly illustrate the change in the mechanical properties induced by compacting. First of all the standard deviation of every parameter of the non-compacted electrodes far exceeds the standard deviation of the compacted electrode. This means the coating becomes homogeneous according to its plastic and elastic deformation behaviour. Moreover, compaction of electrodes reduces the extent of plastic deformation significantly. A reduction of about 11.5 times compared to the non-compacted electrode was achieved, while the elastic properties of the coating almost remain constant after compaction. A change of only 1.35 times can be observed. Thus, the change in total deformation energy can be attributed to the minimization of plastic deformations. This behaviour is well summarized by the ratio of plastic to elastic deformation shown in Table 2. Plastic deformations are irreversible and denote a permanent loss of contact between the active material particles, whereas elastic deformations are reversible and therefore important for a good cycle stability. Thus electrode compaction promotes homogeneous and elastic film properties, which are essential for good cycle stability and high rate capabilities.

In order to quantitatively evaluate the effect of compaction on the electrochemical electrode properties dried electrodes were compacted using a hydraulic press by applying different pressures between 0 and 867 MPa. The SEM micrographs of the electrodes

Table 2
Deformation energies and related mechanical properties of compacted and non-compacted NCA electrodes.

	Total deformation energy [pJ]	Plastic deformation energy [pJ]	Elastic deformation energy [pJ]	Ratio ductile/ elastic	Indentation depth [nm]	Maximum indentation force [μN]
Non-compacted electrode (**250 μm wet film**)						
Average	4821	4043	778	5.16	1670	7999
Standard deviation	2665	2445	346	2.65	948	0.41
Compacted electrode (**250 μm wet film**)						
Average	926	351	574	0.60	372	7999
Standard deviation	175	147	37	0.23	107	0.37

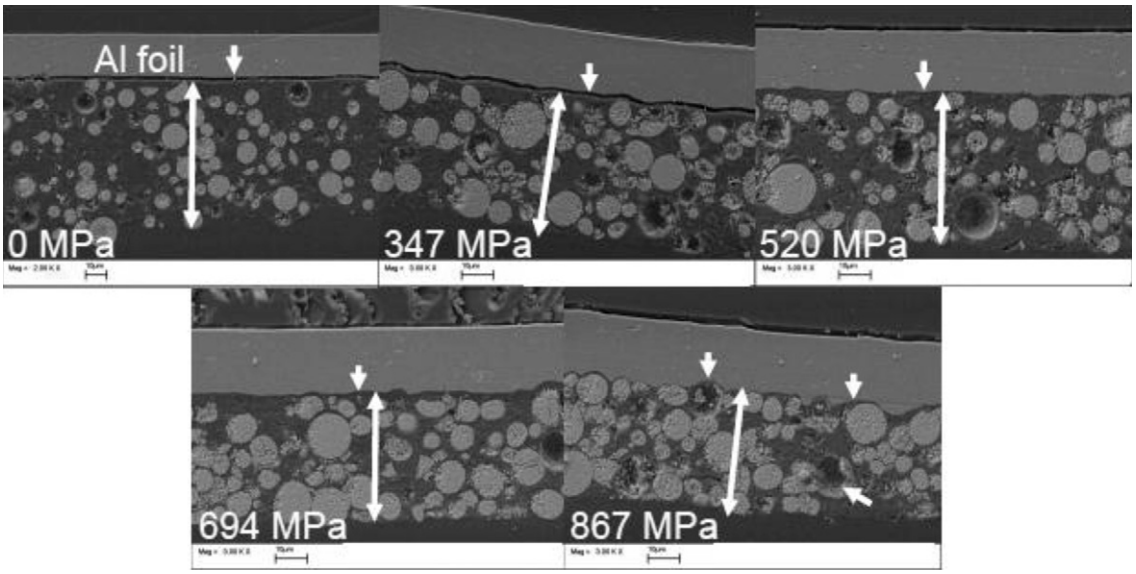

Fig. 6. Cross-section SEM images of an electrode layer compacted at different pressures. The layer composition was: 84 wt.% NCA, 4 wt.% Super P, 4 wt.% SFG6 and 8 wt.% PVdF-binder.

are depicted in Fig. 6. Compression increased significantly both the electrode density and the adhesion to the aluminium current collector. At the same time the electrode thickness decreased (see Fig. 7a). Similar results were observed when compressing negative electrodes [19,20].

Non-compacted electrodes show a poor adhesion to the aluminium foil and relatively low density. When applying 347 MPa or more the electrodes gained in density and showed a slightly better adhesion to the current collector. The tape test confirmed these results. However, above 694 MPa a certain penetration of the electrode mass into the foil can be observed. In general this improves the electronic contact between electrode and aluminium current collector and have a beneficial influence by minimising the resistance [21]. However, the mechanical stress at the contact points may enhance the sensitivity of the aluminium foil to corrosion. This might become a problem if cycling for a long time. At too high pressures a deterioration of the grain architecture of the active mass may occur with a possible disconnection of the crystallites. Further experiments are required in order to prove this.

Fig. 7a shows the correlation between the layer thickness and the applied pressure. A steep decrease in the electrode thickness of about 20 μm can be seen when applying a pressure of 347 MPa, in comparison to the non-compacted electrodes. A further decrease takes place at higher pressures, although less significant – the difference between 347 MPa and 867 MPa is not more than 10 μm.

The influence of the applied pressure onto both cycle stability at a relatively low current (C/5) and rate capability is demonstrated in Fig. 7b and c. The cycleability of the NCA electrodes seems not to depend on the compacting pressure. However, the non-pressed electrodes and those pressed at less than 520 MPa deliver less capacity than the other (ca. 6% less). On contrary, the rate capability improves considerably for the compacted electrodes in comparison to the untreated ones. The non-compacted electrodes show a drastically drop in the capacity at C-rates as high as 1C and deliver no capacity at C-rates higher than 2C. In the case of the compacted electrodes, the applied pressure improves both the contact between the particles of active material and between the electrode and current collector. This improves the overall electronic conductivity of the electrode and leads to a better high-current capability. When cycling again at relative low currents – i.e. C/5 (see cycles 51–60 in Fig. 7c), the non-compacted and the electrodes compacted at 347 MPa show a pronounced capacity fading in comparison to the capacity in the first 10 cycles. This can be due to a poor contact electrode/current collector, which could get worse during cycling.

Electrodes compacted at pressures between 520 MPa and 867 MPa show no significant differences in their electrochemical behaviour – i.e. the discharge capacities have similar values – even though their thicknesses decreased from 45 μm to about 38 μm. However at pressures higher than 694 MPa the oxide particles can suffer certain damages as well as the aluminium collector. This can be very well seen in Fig. 6 and it has been explained above. Another problem which can occur is a decrease in the porosity of the electrodes. This can negatively influence the ion transport through the electrode and thus the electrochemical performances [22]. As illustrated above, a certain degree of compaction is essential to compensate induced mechanical stresses during cycling in order to reach good cycle stability and high rate capabilities. The authors suggest an optimum of 520–694 MPa. Thereby the problems of possible deterioration of the oxide particles and/or of the current collector, with their potential impact on the electrochemical performance of the electrodes, can be as well avoided.

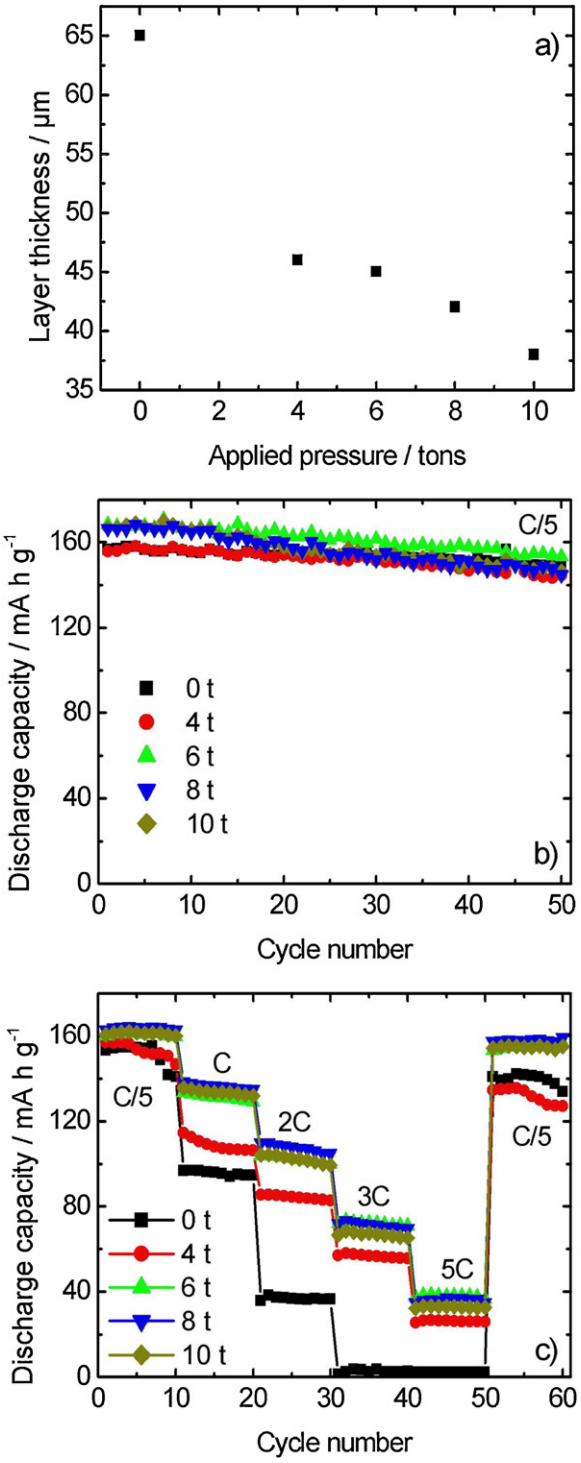

Fig. 7. (a) Variation of the layer thickness for an NCA electrode layer with the compacting pressure. The layer had an initial thickness of 250 µm (wet); (b) cycling stability at C/5 and (c) rate performance of the NCA-electrodes compacted at different pressures. Layer composition was the same as for the electrodes depicted in Fig. 6.

3.3. *Effect of the conductive additive type and mixing ratio on the dispersing behaviour and on the electrochemical performance of the electrodes*

To illustrate the effect of the conductive agents on the dispersing behaviour of the slurry and on the electrochemical performance of the electrodes, the two different conductive agents (Super P and graphite) were mixed in different ratios, while the active material and binder contents were maintained constant at 84 wt.% and 8 wt.%, respectively (see Table 3 for the exact composition of the mixtures).

Table 3
Composite slurries with different contents of conductive agents.

	Slurry 1	Slurry 2	Slurry 3	Slurry 4	Slurry 5
NCA [wt.%]	84	84	84	84	84
Super P [wt.%]	0	2	4	6	8
SFG6 [wt.%]	8	6	4	2	0
PVdF [wt.%]	8	8	8	8	8

Table 4
Different parameters obtained from the analysis: N is the number of pores analysed. μ, σ and β are the expected size value for a circular pore, its variance and skewness respectively obtained fitting the pore size distribution with a lognormal function [3]. ϕ_0 is the surface porosity obtained by SEM images analysis and k is the uniaxial compaction coefficient.

Active materials	N	μ [µm]	σ [µm]	β	ϕ_0	k [µm^{-1}]
0%SupP, 8%SFG6	–	–	–	–	0.000	0.220
2%SupP, 6%SFG6	1791	0.4(1)	0.1(1)	0.0	0.003	0.220
4%SupP, 4%SFG6	2341	0.5(1)	0.1(1)	2.1(3)	0.009	0.240
6%SupP, 2%SFG6	3918	0.5(1)	0.1(1)	2.1(3)	0.017	0.086
8%SupP, 0%SFG6	7780	0.5(1)	0.1(1)	2.2(3)	0.021	0.108

Fig. 8 shows SEM micrographs as well as the surface porosity of composite electrodes containing Super P and SFG6 in different ratios. There is a direct correlation between the amount of Super P and the homogeneity of the electrodes: the higher the amount of Super P, the better the homogeneity. This could be due to the morphology of carbon black, with small particles having a diameter of 40 nm which can distribute better between the active material particles. The graphite particles are much bigger (D_{50} = 3.5 µm) and have a flake-like shape. Therefore they cannot be so homogeneously dispersed into the composite electrode. This can be very well seen in the SEM image in Fig. 8a, showing an electrode containing only graphite as conductive agent. Only some NCA particles can be observed, most of them are covered by graphite flakes. Fig. 8c shows electrodes containing Super P and graphite in a 1:1 ratio, and Fig. 8e electrodes with Super P as the unique conductive agent. The Super P particles are better distributed in comparison to the graphite flakes and can therefore ensure a better electrical contact between the oxide particles. Increasing amount of Super P enhances at the same time gradually the surface porosity of the composite electrodes up to 0.021 for the pure Super P electrode (see Fig. 8).

By looking at the 3D images of the electrode with Super P as the unique conductive agent one can see significant cracks on the electrode surface (Fig. 9), which could influence the lifetime of the electrode.

In addition, the volumetric porosity trend for the electrodes with different ratios of Super P and graphite are performed in Fig. 10 by using following formula [23]:

$$\phi = \frac{w_{\text{wet}} - w_{\text{dry}}}{\rho} \frac{1}{V_{\text{tot}}} \tag{5}$$

where w_{wet} and w_{dry} are the electrode weight before and after wetting, ρ is the density of the electrolyte used for wetting the electrodes (0.28 g cm^{-3}) and V_{tot} is the total electrode material volume. The experiment was performed in the glove box at low pressure (1–3 mbar). The exact values can be taken from Table 4. It shows that the reachable depth for the electrolyte in the electrode composite increases with increasing the Super P content. Thus, a better electrochemical performance at high C-rates can be expected.

The electrodes were then tested regarding their electrochemical performances. Fig. 11a depicts the cycling stability at C/5.

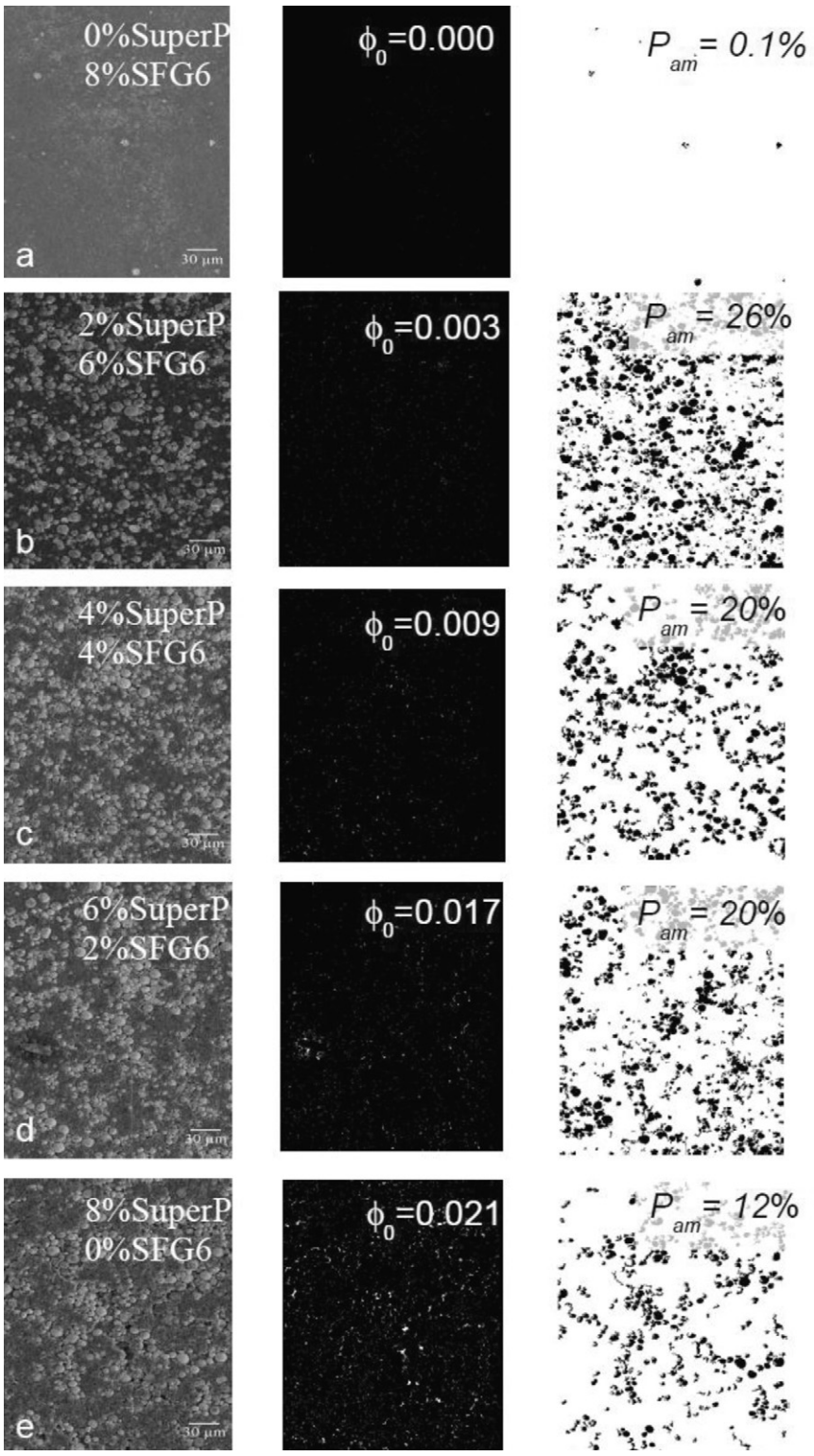

Fig. 8. On left side: SEM images of the electrodes with different amounts of conductive agents; the images in the center and left side represent the pores (white spots) and the active material (black spots) obtained from the images analysis, respectively. The insets ϕ_0 illustrate the surface porosity values obtained from images analysis while P_{am} is the percentage of active material area in the image.

Fig. 11b shows the discharge capacities obtained when charging at C/5 and discharging at different currents between C/5 and 5C. The electrodes containing graphite as the only conductive agent showed at C/5-rates a discharge capacity of only 100 mAh g^{-1}, which is about 63% from the capacity delivered by the other three kinds of electrodes. Graphite alone seems not to be able to ensure a good contact between the particles. All the electrodes containing Super P as conductive agent, alone or as mixed with graphite, deliver a relatively high discharge capacity of about 160 mAh g^{-1}. The cycling stability of the electrodes containing 4 wt.% or more Super P is considerably higher than that of the electrodes with less or no Super P. A content of carbon black between 4 and 8 wt.%

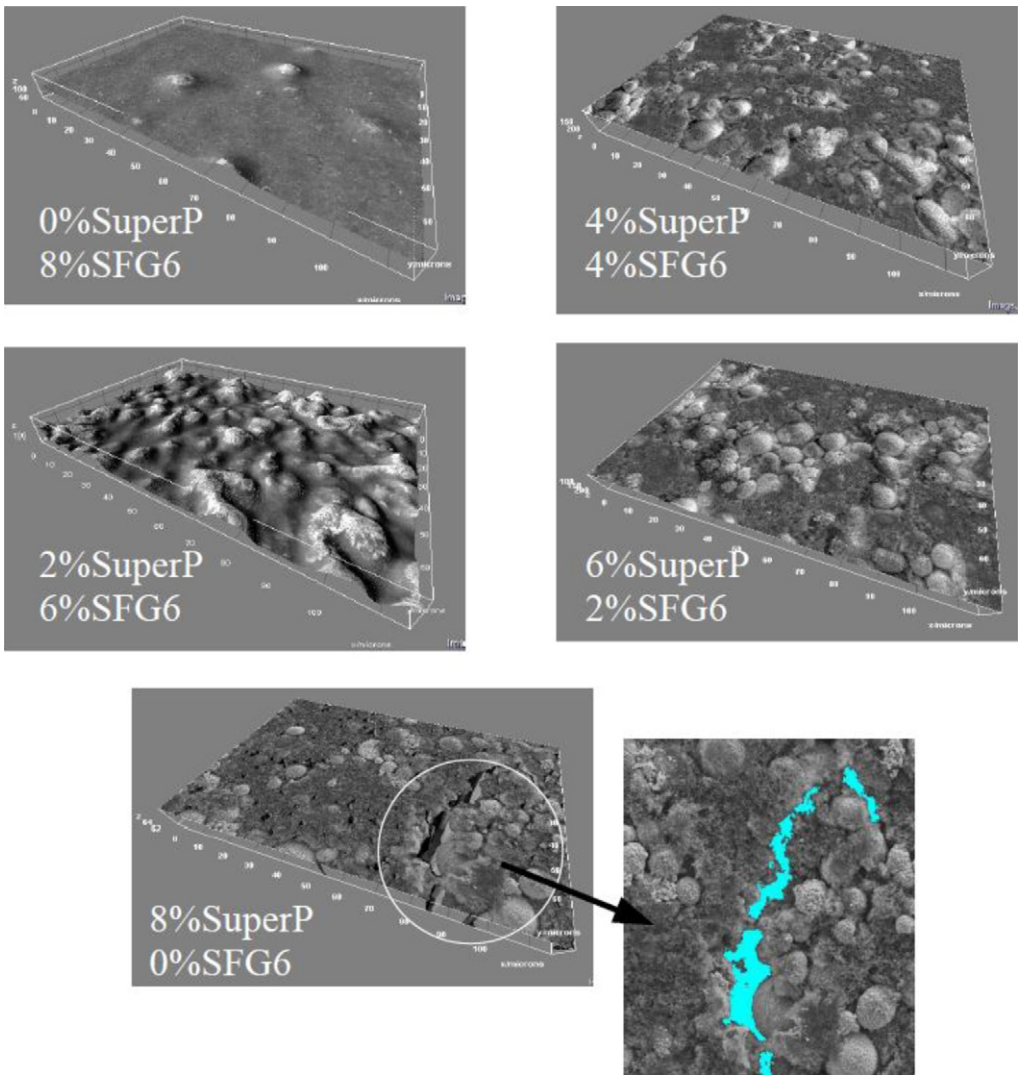

Fig. 9. 3D images (ImageJ program) obtained by different amount of conductive material electrodes SEM images.

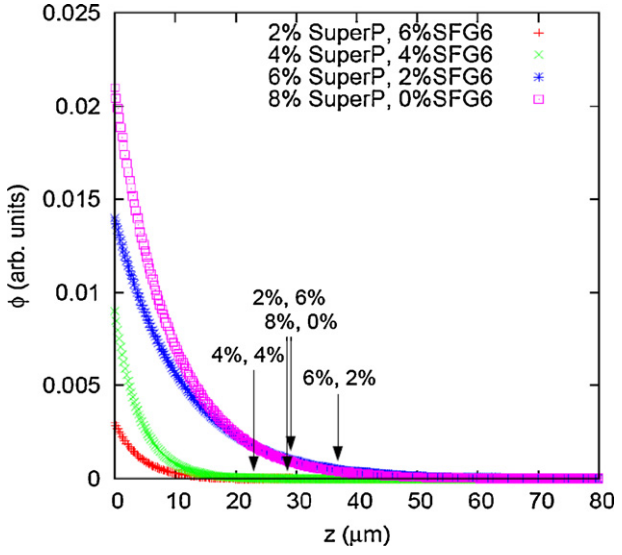

Fig. 10. Volumetric porosity trend obtained for the different conductive material amounts. The arrows show the thickness values of the electrodes obtained after pressing (694 MPa).

Table 5
Capacity retention at different Super P contents in the electrode mixtures.

Mixture	Super P content [%]	Capacity retention (versus discharge capacity at C/5) [%]	
		1C	5C
1	0	57	7.5
2	2	79	14.5
3	4	89	40
4	6	92	53
5	8	92	75

ensures a good homogeneity of the electrodes which can be considered responsible for the improved cycleability.

The effect of Super P becomes even more significant when cycling the electrodes at C-rates higher than 1C. The discharge capacities are depicted in Fig. 11b. Electrodes with no/only 2 wt.% Super P deliver almost no capacity at currents as high as 5C. NCA electrodes containing Super P as unique conductive agent show an excellent rate capability, with discharge capacities at 5C as high as 120 mAh g^{-1}. This corresponds to capacity retentions of 75% if taking the discharge capacity at C/5 as reference (see Table 5).

However the electrodes containing more than 4 wt.% Super P suffer from a lower energy density when compared to the other electrodes. In spite of their excellent electrochemical performances

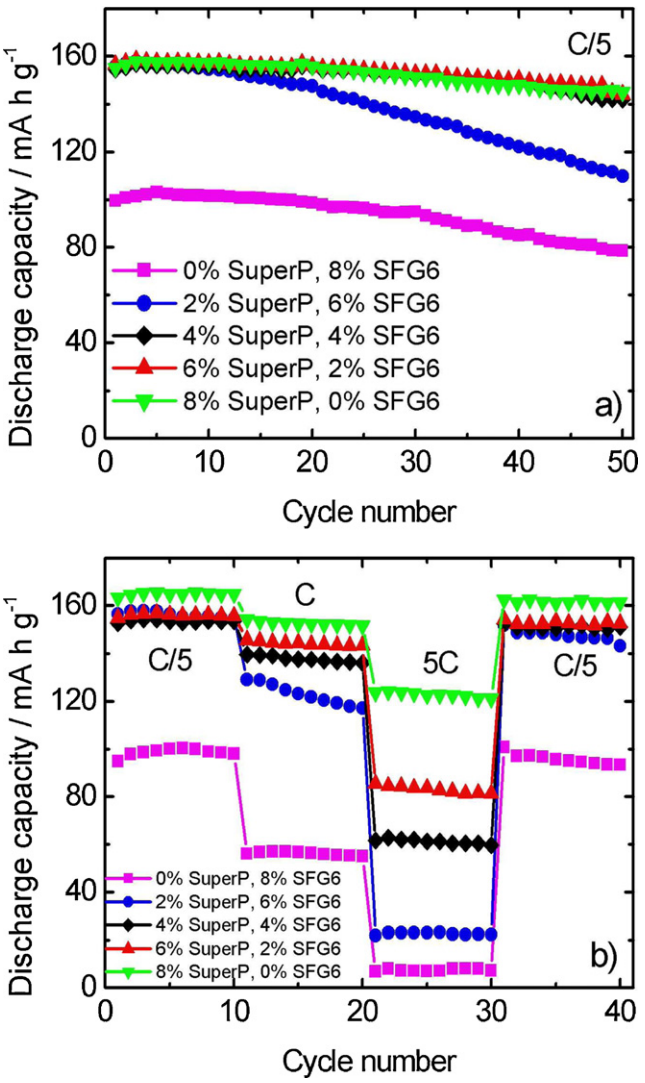

Fig. 11. Characterization of the NCA composite electrodes with Super P and graphite in different ratios: (a) cycling stability at C/5-rate and (b) rate capability: charge C/5, discharge C/5, C, 5C and back to C/5.

at high C-rates, electrodes with a relatively high Super P content might not be suitable for high energy applications. An increase in the electrode thickness followed by an appropriate compacting can be a possible solution for obtaining a higher energy density.

4. Conclusions

Electrode preparation has been neglected in most of the studies where accent has been put on finding new, better performing electrode materials. The present work has demonstrated the significant influence of the electrode preparation on the electrochemical performances of the NCA-based cathode composite electrodes.

The selection of the conductive additives, as well as the mixing ratio has been found to have a great impact on the dispersing behaviour of the slurry and thus on the homogeneity of the electrodes. Super P and synthetic graphite were chosen for this study, since they are two of the most used conductive additives for Li-ion batteries electrodes. The rate capability of the NCA electrodes has been pronouncedly improved by the addition of Super P. Electrodes containing only Super P as conductive agent deliver the best capacity values – i.e. the capacity retention at 5C was 75%. Electrodes with graphite as the unique conductive additive are less homogeneous and show poor electrochemical performances. Even at relatively low C-rates – i.e. C/5 – they are able to deliver only about 63% of the capacity of the electrodes containing Super P.

However, the higher the Super P amount, the lower the energy density of the electrodes. In spite of their excellent electrochemical performances especially at C-rates as high as 5C, the electrodes with a high amount of Super P might need further improvements in order to become suitable for high energy applications.

Different wet thicknesses (resulting also in different loadings of the electrodes) and degree of compacting have been found as further significant parameters influencing the electrochemical behaviour.

As expected, the electrode loading density has been improved by increasing the thickness. At relatively low current densities no significant differences between the NCA electrodes with different loadings have been observed.

On contrary, at higher C-rates electrodes with lower loading deliver significantly more capacity than those with higher loading. The lower rate capability of the latter can be explained by the longer electron transport paths within the electrode. This results in a higher number of contact resistance points leading to a higher overall electronic resistance. For very high C-rates electrolyte diffusion may become significant and lithium exhaustion can be the rate limiting factor.

Compacting has been proven to be an efficient and relatively easy method for improving the electrochemical performances of the electrodes. By electrode compaction the adhesion to the current collector as well as the homogeneity of the coating itself are significantly improved. This improves the overall electronic conductivity of the electrode and leads to a better high-current capability. Moreover, through compaction the elastic deformation becomes predominant against plastic deformation, thus improving the cycling stability of the electrode. However, too high pressures can result in damages of both active material particles and aluminium current collector. Also, the porosity of the electrodes and thus the ion transport can be thereby negatively influenced.

Cathode design has been demonstrated to be an important issue for enhancing battery performances in terms of both energy density and electrochemistry. There are still other parameters interfering in the electrode preparation which can be investigated and improved. This could allow for the manufacturing of electrodes which can fulfil the continuously increasing requirements for different applications.

Acknowledgement

Financial support from the Deutsche Forschungsgemeinschaft (DFG, Functional materials and material analysis for lithium high power batteries) is gratefully acknowledged.

References

[1] K. Mizushima, P.C. Jones, P.J. Wiseman, J.B. Goodenough, Mater. Res. Bull. 15 (1980) 783.
[2] C. Delmas, I. Saadoune, Solid State Ionics 53–56 (1992) 370.
[3] A. Funahashi, Y. Kida, K. Yanagida, T. Nohma, I. Yonezu, J. Power Sources 104 (2002) 248.
[4] T. Ohzuku, A. Ueda, M. Kouguchi, J. Electrochem. Soc. 142 (1995) 4033.
[5] C.H. Chen, J. Liu, K. Amine, Abstract 176, ECS Fall Meeting, San Francisco, 2001.
[6] M. Broussely, Ph. Blanchard, Ph. Biensan, J.P. Planchat, K. Nechev, R.J. Staniewicz, J. Power Sources 119–121 (2003) 859.
[7] H. Kaneta, US Patent No. 2006/0188777 A1.
[8] T. Sasaki, et al., US Patent No. 2003/0124423.
[9] T. Manabu, et al., JP Patent No. 2000-030745.
[10] T. Yuji, et al., JP Patent No. 2002-151055.
[11] K.M. Kim, W.S. Joen, I.J. Chung, S.H. Chang, J. Power Sources 83 (1999) 108.
[12] K. Terashita, K. Miyanami, Adv. Powder Technol. 13 (2) (2002) 201.
[13] M.S. Park, Y.J. Lee, Y.S. Han, J.Y. Lee, Mater. Lett. 60 (2006) 3079.
[14] M.E. Rabanal, M.C. Gutierrez, F. Garcia-Alvarado, E.C. Gonzalo, M.E. Arroyo-de Dompablo, J. Power Sources 160 (2006) 523.

[15] Y. Sato, T. Nakano, K. Kobayakawa, T. Kawai, A. Yokoyama, J. Power Sources 75 (1998) 271.
[16] A.B. Abell, K.L. Willis, D.A. Lange, J. Colloid Interface Sci. 211 (1990) 39.
[17] L.F. Athy, Bull. Am. Assoc. Petrol. Geol. 14 (1930) 1.
[18] A.C. Fischer-Cripps, Nanoindentation, 2nd ed., Springer, New York, NY, 2004.
[19] P. Novak, W. Scheifele, M. Winter, O. Haas, J. Power Sources 68 (1997) 267.
[20] K.A. Striebel, A. Sierra, J. Shim, C.W. Wang, A.M. Sasty, J. Power Sources 134 (2004) 241.
[21] M. Gaberscek, J. Moskon, B. Erjavec, R. Dominko, J. Jamnik, Electrochem. Solid-State Lett. 11 (2008) A170.
[22] Y.H. Chen, C.W. Wang, X. Zhang, A.M. Sastry, J. Power Sources 195 (2010) 2851.
[23] L. Ottaviano, A. Filipponi, A. Di Cicco, Phys. Rev. B 49 (1994) 11749.